

Differentiable Scene Graphs

Moshiko Raboh^{1*}, Roei Herzig^{1*}, Gal Chechik^{2,3}, Jonathan Berant^{1,4}, Amir Globerson¹

¹Tel Aviv University, ²Bar-Ilan University, ³NVIDIA Research, ⁴AI2

¹{mosheraboh@mail, roeiherzig@mail, jobberant@cs, gamir@post}.tau.ac.il

²{gal.chechik}@biu.ac.il

Abstract

Understanding the semantics of complex visual scenes involves perception of entities and reasoning about their relations. Scene graphs provide a natural representation for these tasks, by assigning labels to both entities (nodes) and relations (edges). However, scene graphs are not commonly used as intermediate components in visual reasoning systems, for two complementary reasons. First, training models to map images to scene graphs requires prohibitive manual annotation, and results in graphs that often do not match the needs of a downstream visual reasoning application. Second, using these discrete graphs as an intermediate latent representation results in a non-differentiable function that is difficult to optimize.

Here we propose *Differentiable Scene Graphs (DSGs)*, an image representation that is amenable to differentiable end-to-end optimization, and requires supervision only from the downstream tasks. DSGs provide a dense representation for all regions and pairs of regions, investing model capacity on the important aspects of the image. We describe a multi-task objective function that allows us to learn this representation from indirect supervision only, provided by the downstream task. We evaluate our model on the challenging task of identifying referring relationships, and show that training DSGs using our multi-task objective leads to new state-of-the-art performance.

1. Introduction

Understanding the full semantics of rich visual scenes is a complex task that involves detecting individual entities, as well as reasoning about the joint combination of the entities and the relations between them. To represent entities and their relations jointly, it is natural to view them as a graph, where nodes are entities and edges represent relations. Such representations are often called *Scene Graphs (SGs)* [16]. Because SGs allow to explicitly reason about

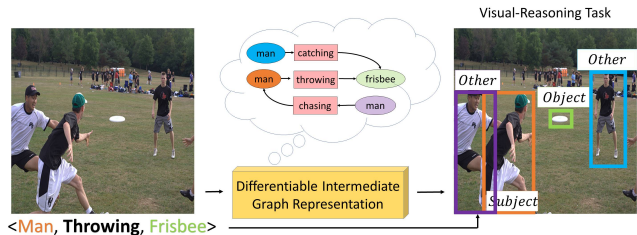


Figure 1. **Differentiable Scene Graphs**: an intermediate “graph-like” representation that provides a distributed representation for each entity and pair of entities in an image. Differentiable scene graphs can be learned with gradient descent in an end-to-end manner from the supervision for a downstream visual reasoning task only (referring relations here).

images, substantial efforts have been made to infer them from raw images [15, 16, 37, 24, 43, 11, 44].

While scene graphs have been shown to be useful for some tasks [15, 16, 13], using them as a component in a visual reasoning system is challenging: (a) Because scene graphs are discrete and non-differentiable, it is difficult to learn them end-to-end from a downstream task. (b) The alternative is to pre-train SG predictors separately from supervised data, but this requires arduous and prohibitive manual annotation. Moreover, pre-trained SG predictors have *low coverage*, because the set of labels they are pre-trained on rarely fits the needs of a downstream task. For example, given an image of a parade and a question “*point to the officer on the black horse*”, that horse might not be a node in the graph, and the term “officer” might not be in the vocabulary. Given these limitations, it is an open question how to make scene graphs useful for visual reasoning applications.

In this work, we describe *Differentiable Scene-Graphs (DSG)*, which address the above challenges (Figure 1). DSGs are an **intermediate representation trained end-to-end from the supervision for a downstream reasoning task**. The key idea is to relax the discrete properties of scene graphs such that each entity and relation is described with a dense differentiable descriptor.

*Equal Contribution.

To evaluate DSGs, we tackle the task of resolving *referring relationships* (RR) [20], where given an image and a $\langle \text{subject}, \text{relation}, \text{object} \rangle$ query, a model must find the subject and object bounding boxes that participate in the specified relation. The advantage of RR is it requires very little *language understanding* compared to other visual reasoning tasks (e.g., VQA [1] or referring expressions [17, 19]), focusing on the visual aspect.

We train an RR model with DSGs as the central component. The latent DSG representation is trained using a multi-task objective that includes (a) the end-to-end referring relationship objective, as well as (b) auxiliary objectives that are based on labels for a small subset of the objects and relations, given as part of the RR dataset. We evaluate our approach on three standard RR datasets: Visual Genome [21], VRD [25] and CLEVR [14], and find that DSGs substantially improve performance compared to state-of-the-art approaches [25, 20]. Moreover, we find that our proposed multi-task objective, which explicitly considers the partial supervision provided in the training set, clearly contributes to the improved performance.

To conclude, our novel contributions are: (1) A new *Differentiable Scene-Graph* representation for visual reasoning, which captures information about multiple entities in an image and their relations. We describe how DSGs can be trained end-to-end with a downstream visual reasoning task without direct supervision of pre-collected scene-graphs. (2) A new architecture for the task of referring relationships, using a DSG as its central component. (3) New state-of-the-art results on the task of referring relationships on the Visual Genome, VRD and CLEVR datasets.

2. Differentiable Scene Graphs

A scene graph represents entities and relations in an image as a set of nodes and edges. A “perfect” scene graph (representing all entities and relations) captures most of the information needed for visual reasoning, and thus should be useful as an intermediate representation. However, learning to predict “perfect” scene graphs for any downstream task is unlikely due to the aforementioned challenges.

Instead, we propose an intermediate representation, termed “Differentiable Scene Graph” Layer (DSG), which captures the information in a scene graph but can be trained end-to-end in a task-specific manner (Fig. 2). A DSG contains a dense distributed representation vector for each detected entity (termed *node descriptor*) and each pair of entities (termed *edge descriptor*). These representations are themselves learned functions of the input image, as we explain in Sec. 4.2. The DSG is then used as input to a visual-reasoning module (e.g., referring relations in our case).

The advantages of our approach are:

Differentiability: Because node and edge descriptors are differentiable functions of detected boxes, and are fed into

a differentiable reasoning module, the entire pipeline can be trained with gradient descent.

Dense Coverage: By keeping dense descriptors for nodes and edges, the DSG succeeds to keep dense information about possible semantics of nodes and edges. Instead of committing too early to hard sparse representations, it keeps a more flexible representation that better fits a series of downstream tasks.

Indirect supervision: Training data that is available for downstream tasks often contains partial annotation of an image, such as the label for some of the entities. We show that such information can be used to train the DSG in a multi-task setting.

Holistic Representation: DSG descriptors are computed by integrating global information from the entire image using graph neural networks (see Sec 4.2), which increases the accuracy of each descriptor.

3. Referring Relationship: The Learning Setup

In the referring relationship task [20] we are given an image I and a subject-relation-object query $\langle s, r, o \rangle$. The goal is to output two sets of bounding boxes \mathcal{B}_s and \mathcal{B}_o , where each bounding box $b_s \in \mathcal{B}_s$ corresponds to a subject entity s and each bounding box $b_o \in \mathcal{B}_o$ corresponds to an object entity o that participates in the ordered relation r in the image I .¹ See Fig. 1 for a sample query and expected output.

Following [20], we will focus on training a referring relationship predictor from labeled data. Namely, we will use a training set consisting of images, queries and the correct boxes for these queries. We denote these by $\{(I_j, q_j, (\mathcal{B}_j^s, \mathcal{B}_j^o))\}_{j=1}^N$. Also following [20], we assume that the vocabulary of the query components (subject, object and relation) is fixed.

We next formally describe the architecture of our model.

4. Model

The key element in our approach is the use of a differentiable scene-graph representation for answering visual-reasoning tasks. In what follows we describe how this representation is calculated, and how it is trained using partial supervision with a multi-task objective.

4.1. Model Components

At a high level, the model works as follows (Fig. 2). It first extracts bounding boxes from the image. Next, it creates a scene-graph over these bounding boxes. A scene-graph here refers to a set of distributed representations for all the bounding boxes, as well as representations of relations for each pair of bounding boxes. Finally, the scene-

¹There can be multiple boxes, because an image may contain multiple instances of “man kicking ball”.

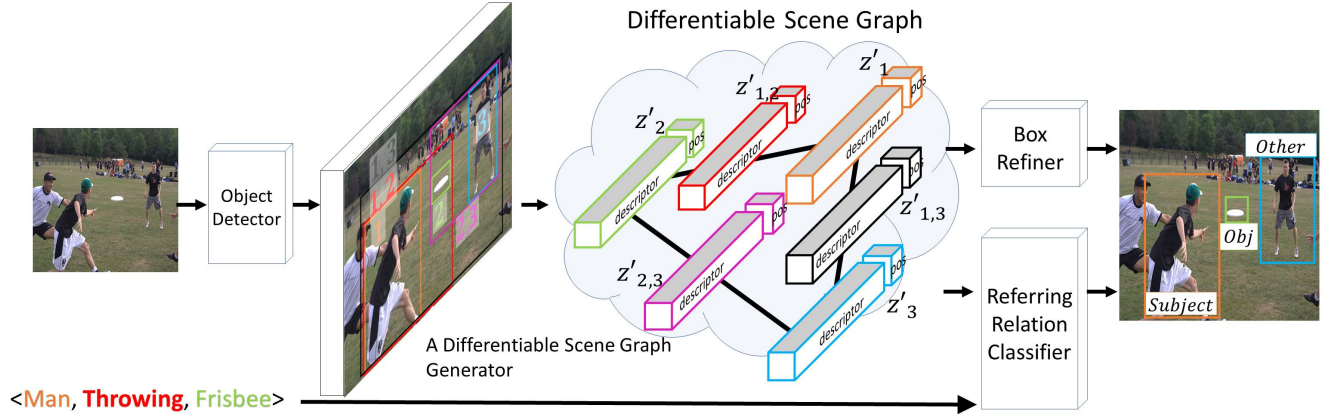


Figure 2. **The proposed architecture.** The input consists of an image and a relationship query triplet $\langle \text{subject}, \text{relation}, \text{object} \rangle$. (1) A detector produces a set of bounding box proposals. (2) An *RoiAlign* layer extracts object features from the backbone using the boxes. In parallel, every pair of box proposals is used for computing a union box, and pairwise features extracted in the same way as object features. (3) These features are used as inputs to a Differentiable Scene-Graph Generator Module which outputs the Differential Scene Graph, a new and improved set of node and edge features. (4) The DSG is used for both refining the original box proposals, as well as a Referring Relationships Classifier, which classifies each bounding box proposal as either Subject, Object, Other or Background. The ground-truth label of a proposal box will be *Other* if this proposal is involved in another query relationship over this image. Otherwise the ground truth label will be *Background*.

graph representation is used as input for a model that answers the query. Namely, the model labels each box as Subject, Object, Other and Background.²

Object Detector - The first stage is to detect candidate entities in the image using a standard region proposal network (RPN) [32]. The RPN output is a set of bounding boxes which are assumed to contain entities of interest. We denote the bounding boxes for these by b_1, \dots, b_B .³ For each bounding box, we also extract the corresponding feature vector and denote it by f_i . Finally, we denote the concatenation of f_i and b_i by $z_i = [f_i; b_i]$

Relation Feature Extractor - Next, we extract features that will be useful for representing relations between entities in two bounding boxes. Consider two bounding boxes b_i and b_j . In order to reason about the relation between these, it is useful to consider the smallest box that contains both these boxes. We denote this “relation box” box by $b_{i,j}$. Since $b_{i,j}$ is also in the set of regions considered by the RPN, we have a corresponding feature vector $f_{i,j}$. Finally, we denote the concatenation of $f_{i,j}$ and $b_{i,j}$ by $z_{i,j}$.

Differentiable Scene-Graph Generator - The goal of the Differentiable Scene-Graph Generator model is to transform the above features z into a representation of the underlying scene graph. Namely, into a set of vectors representing the entities and relations in the image, and taking into

²The label “Other” refers to a case where we know a box contains an entity that is not the given subject or object. The label “Background” refers to a case where we cannot determine if the box describes an entity at all.

³The number of boxes may vary between images, but we use the same B for all for simplicity.

account image context.⁴ We denote the vector for the i^{th} entity by z'_i and for the relation between entity i and entity j by $z'_{i,j}$. To obtain these vectors, we can use any architecture for scene-graph prediction that outputs a representation for entities and relations. Here we use the model proposed by [11], which takes as input initial entity representations z_i and initial relation representations $z_{i,j}$ and uses a graph neural network to transform these into the desired z' representation. See Sec. 4.2 for details on this network.

Referring Relationship Classifier - Given a scene-graph representation, we can use it for answering referring relationship queries. Recall that the output of an RR query $\langle \text{subject}, \text{relation}, \text{object} \rangle$ should be bounding boxes in the query relation. Our model has already computed B bounding boxes b_i , as well as representations z'_i for each box. We next use a prediction model $F_{RRRC}(z'_i, q)$ that takes as input features describing a bounding box and the query, and outputs one of four labels $\{\text{Subject}, \text{Object}, \text{Other}, \text{Background}\}$ where *Other* refers to a bounding box which is not the query Subject or Object and *Background* refers to a false entity proposal. Denote the logits generated by this classifier for the i^{th} box by $r_i \in \mathbb{R}^4$. The output set \mathcal{B}_s (or \mathcal{B}_o) is simply the set of bounding boxes classified as Subject (or Object). See Sec. 6.1 for further implementation details.

Bounding Box Refinement - The Differentiable Scene-Graph can also be used for further refinement of the

⁴See description of “Scene-Graph Labeling Loss” in Sec. 5 for information on how to extract a scene graph from these vectors.

bounding-boxes generated by the RPN network. The idea is that additional knowledge about image context may help to improve the coordinates of a given object. This is done via a network $F_{BR}(b_i, z'_i)$ that takes as input the RPN box coordinates and a differentiable representation z'_i for box i , and outputs new bounding box coordinates. See Fig 6 for an illustration of box refinement and see Sec. 6.1 for further implementation details.

4.2. The Scene Graph Generator

We next describe the module that takes as input features z_i and $z_{i,j}$ extracted by the RPN and outputs a set of vectors z'_i, z'_{ij} corresponding to Differentiable Scene-Graph over entities and relationships in the image. For this model, we use the Graph Permutation Invariant (GPI) architecture introduced in [11]. A key property of this architecture is that it is invariant to permutations of the input that do not affect the labels.

The GPI transformation is defined as follows. First, the set of all input features is summarized via a permutation-invariant transformation into a single vector g :

$$g = \sum_{i=1}^n \alpha(z_i, \sum_{j \neq i} \phi(z_i, z_{i,j}, z_j)) \quad (1)$$

Here α and ϕ are fully connected networks. Then the new representations for entities and relations are computed via:

$$z'_k = \rho^{entity}(z_k, g), \quad z'_{k,l} = \rho^{relation}(z_{k,l}, g) \quad (2)$$

where ρ above are fully connected networks. See Sec. 6.1 for further implementation details.

5. Training

We next explain how our model is trained for the RR task, and how we can also use the RR training data for supervising the DSG component. The training loss will be a sum of the following losses. Some of these correspond directly to the referring relationship task, and some to the auxiliary task of DSG labeling.

Referring Relationship Classifier Loss - The *Referring Relationship Classifier* (Sec. 4) outputs logits r_i for each box, corresponding to its prediction (subject, object, etc.). To train these logits, we need to extract their ground-truth values from the training data. Recall that a given image in the training data may have multiple queries, and so may have multiple boxes that have been tagged as subject or object for the corresponding queries. To obtain the ground-truth for box i and query $q = \langle s, r, o \rangle$ we take the following steps. First, we find the ground-truth box that has maximal overlap with box i . If this box is either a subject or object for the query q , we set r_i^{gt} to be Subject or Object respectively. Otherwise, if the overlap with a ground-truth

box for a different image-query is greater than 0.5, we set $r_i^{gt} = \text{Other}$ (since it means there is some other entity in the box), and we set $r_i^{gt} = \text{Background}$ if the overlap is less than 0.3. If the overlap is in $[0.3, 0.5]$ we do not use the box for training. For instance, given a query $\langle \text{woman}, \text{feeding}, \text{giraffe} \rangle$ with ground-truth boxes for “woman” and “giraffe”, consider the box in the RPN that is closest to the ground-truth box for “woman”. Assume the index of this box is 7. Similarly, assume that the box closest to the ground-truth for “giraffe” has index 5. We would have $r_7^{gt} = \text{Subject}$, $r_5^{gt} = \text{Object}$ and the rest of the r_i^{gt} values would be either Other or Background. Given these ground truth values, the Referring Relationship Classifier Loss is simply the sum of cross entropies between the logits r_i and the one-hot vectors corresponding to r_i^{gt} .

Scene-Graph Labeling Loss - As mentioned earlier, we can also use the ground-truth data as partial labels for training the DSG. Consider again the query $\langle \text{woman}, \text{feeding}, \text{giraffe} \rangle$, where the index for the box in the RPN that is closest to the ground-truth box for “woman” is 7, and the index of the box closest to the ground-truth for “giraffe” has index 5. The box corresponding to “woman” has a DSG representation vector z'_7 . It makes sense to require that the label “woman” should be inferred from the vector z'_7 . To enforce this, we train a classifier from z' to the set of entity labels, and add a loss to maximize its accuracy with respect to the ground truth. Similarly, recall that we have a representation $z'_{i,j}$ for relations in the DSG. Thus we would want the label “feeding” to be inferred from the vector $z'_{7,5}$.

The above approach is implemented as follows. Denote by E the number of entity values (e.g., “horse”, “cat”, “cow” etc.) and R the number of relation values (e.g., “holding”, “kicking” etc.). We construct two classifiers. The first is a linear classifier that takes as inputs a vector z'_i and outputs logits $v_i \in \mathbb{R}^E$. The second is a linear classifier that takes as input a vector $z'_{i,j}$ output logits $v_{i,j} \in \mathbb{R}^R$. For each query, we have three ground-truths for the above logits. Thus, our DSG Labeling Loss is a sum of cross-entropy loss for the three ground-truth labels (one for the subject, one for the object and one for the relation).

Fig. 3 shows an example of a Scene-Graph produced by our model, trained using this loss. It can be seen that the predicted graph is indeed largely correct despite the fact that it was trained from partial supervision only.

Object Detector Loss - The output of the RPN is a set of bounding boxes. The ground-truth contains boxes that are known to contain objects. The goal of this loss is to encourage the RPN to include these boxes as proposals. Concretely, we use a sum of two losses: First, an RPN classification loss, which is a cross entropy over RPN anchors where proposals of 0.8 overlap or higher with the ground truth boxes were considered as positive. Second, an RPN box regression loss which is a smooth L1 loss between the

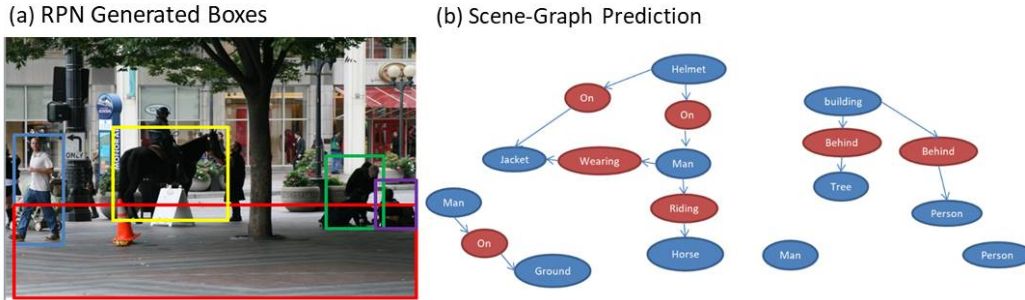


Figure 3. Detailed example of DSG based prediction. Applying the RPN to this image results in 28 boxes. In (a) we show five of these, which received the largest weight in the attention model within the DSG generator (Sec. 4.2). As mentioned in Sec. 5 in “Scene-Graph Labeling Loss” we can use the DSG for generating a labeled scene graph, corresponding to a fixed set of entities and relations. (b) shows this scene graph (i.e., the output of the classifiers predicting entity labels and relations), restricted to the largest confidence relations. It can be seen that most relations are correct, despite not having trained this model on complete scene graphs.

ground-truth boxes and proposal boxes.

Box Refinement Loss - Recall that we have a *Bounding Box Refinement* component. As with the Object Detector Loss above, we add a smooth L1 loss between the refined boxes and the ground truth ones. Thus, we have two loss terms for the bounding boxes generated in the network: the first one for the boxes generated by the RPN, and the second one for the boxes generated by the refinement. Our ablation study shows that using the refined boxes does improve performance.

6. Experiments

In the following sections we provide details about the model implementation, datasets, training, baselines models, evaluation metrics, model ablations and results.

6.1. Model Details

The model in Sec. 4.1 is implemented as follows.

Object Detector and Relation Feature Extractor. For object detection, we used Faster-RCNN with a 101-layers ResNet backbone. The RPN was trained with anchor scales of $\{4, 8, 16, 32\}$ and aspect ratios $\{0.5, 1, 2\}$. RPN proposals were filtered by non-maximum suppression with IOU-threshold of 0.5 and score higher than 0.8. We use at most 32 proposals per image. Both the entity features f_i and the relation features $f_{i,j}$ are first extracted from the convolutional network feature map by the ROI-Align layer as $7 \times 7 \times 2048$ features. They are then reduced to a $7 \times 7 \times 512$ by convolution layer of size 1×1 and finally reduced to 1×512 by an average pooling layer.

Differentiable Scene-Graph Generator. The three networks ϕ , α and ρ , described in GPI architecture (Sec. 4.2) are two fully-connected layers with 512 hidden units. The output size of ϕ and α is 512, and of ρ is 1024.

Referring Relationship Classifier. The referring relation-

ship classifier F_{RRC} is a fully-connected network with two layers of 512 hidden units each.

Bounding Box Refinement. The box refinement model applies a linear function to z_i to obtain four outputs $[dx, dy, dw, dh]$. Denote the RPN box by $[x, y, w, h]$. The refined box is then: $[dx \cdot w + x, dy \cdot h + y, e^{dw} \cdot w, e^{dh} \cdot h]$ (as in the correction used by Faster-RCNN).

6.2. Datasets

We evaluate the model performance on the task of referring relationships across three datasets, each exhibiting a unique set of characteristics and challenges.

CLEVR [14]: A synthetic dataset generated from scene-graphs with four spatial relations: “left”, “right”, “front” and “behind”, and 48 entity categories. It has over 5M relationships where 33% are ambiguous entities (namely cases where there are multiple entities of the same type in an image).

VRD: The Visual Relationship Detection dataset [25] contains 5,000 images with 100 entity categories and 70 relation categories. In total, VRD contains 37,993 relationship annotations with 6,672 unique relationship types and 24.25 relations per entity category. 60.3% of these relationships refer to ambiguous entities.

Visual Genome: The Visual Genome dataset [21] is the largest public corpus for visual relationships in real images. It contains 108,077 images annotated with bounding boxes, entities and relations. On average, images have 12 entities and 7 relations per image. In total, there are over 2.3M relationships where 61% of those refer to ambiguous entities.

For a proper comparison with previous results [20], we used the data from [20] including the same entity and relation categories, query relationships and data splits.



Figure 4. Qualitative examples demonstrating predictions of our DSG model. **Left Columns:** Examples of correct predictions. **Right Column:** Examples of two failure cases. On the top image, the model incorrectly recognizes a newspaper on the wall as a sign. On the bottom image, the model recognizes a picture on the wall instead of a clock.

6.3. Training Details

Our model was trained using SGD with momentum 0.9 and learning rate 0.01 decaying by a factor of 0.5 every two epochs over Visual Genome and CLEVR and every ten epochs over VRD. The model was trained for 20 epochs over Visual Genome and CLEVR and for 50 epochs over VRD. The detector weights were initialized with an ImageNet pre-trained detector. Each batch includes all the query relationships in a single image. The total loss was set to be a weighted sum of the losses of the following components (see Sec. 5): Object Detector, Referring Relationship Classifier, Box Refinement and Differentiable Scene-Graph Labeling. The weights were set to 1, 0.2, 1 and 0.01 respectively. In order to be comparable to previous works described in Sec. 6.6, only relationships annotated for the referring relationship task were considered in the losses.

6.4. Evaluation Metrics

We compare our model to previous work using the average IOU for subjects and for objects. To compute the average subject IOU, we first generate two $L \times L$ binary attention maps: one that includes all the ground truth boxes labeled as Subject (recall that few entities might be labeled as Subject) and the other includes all the box proposals predicted as Subject. If no box is predicted as Subject, the box with the highest score for the label Subject is included in the predicted attention map. We then compute

the Intersection-Over-Union between the binary attention maps. For a proper comparison with previous work [20], we use $L = 14$. The object boxes are evaluated in the exact same manner.

6.5. Model Ablations

We explored the power of our model through model ablations, comparing the following models:

- (1) DSG: The Differentiable Scene-Graph model described in Sec. 4.1 and trained as described in Sec. 5
- (2) DSG -DSGL: This model is a variant of DSG but without the Differentiable Scene-Graph Labeling Loss (see Sec. 5). This ablation allows us to study the effect of training the Differentiable Scene-Graph component using partial labels.
- (3) DSG -BR: This model is a variant of DSG but replacing the *Box Refinement* component with fine tuning the coordinates of the box proposal using the visual features f_i . This variant allows us to quantify the benefit of refining the box proposals based on the differentiable representation of the scene.
- (4) DSG -SG: A baseline model that does not use the DSG representations at all. Instead, the model includes only Object Detector and a referring relationship classifier. The referring relationship classifier uses the f_i features extracted by the Object Detector instead of the z_i features. This model allows us to quantify the benefit of the differentiable scene representation for referring relationship classification.

	Visual Genome		Average IOU		CLEVR	
	subject	object	subject	object	subject	object
SS [22]	0.399	0.469	0.320	0.371	0.740	0.740
CO [7]	0.414	0.490	0.347	0.389	0.691	0.691
VRD [25]	0.417	0.480	0.345	0.387	0.734	0.732
SASS [20]	0.421	0.482	0.369	0.410	0.778	0.778
DSG -SG	0.412	0.47	0.333	0.366	0.937	0.937
DSG	0.489	0.539	0.4	0.435	0.963	0.963

Table 1. Test set results on the referring relationship task for the baselines in Sec. 6.6, and our Differentiable Scene Graph (DSG) model. Additionally, results are reported on a DSG -SG model (see Sec. 6.5) which classifies the referring relationship directly from the RPN output.

	Average IOU	
	subject	object
DSG -SG	0.405	0.461
DSG -DSGL	0.455	0.511
DSG -BR	0.469	0.519
DSG	0.477	0.528

Table 2. **Model ablations:** Results for DSG variants on the validation set of the Visual Genome dataset. The different models are described in Sec. 6.5.

6.6. Baselines

The Referring Relationship task was introduced recently [20], and the SSAS model was proposed as a possible approach (see below). We report the results for the baseline models in [20]. When evaluating our Differentiable Scene-Graph model, we use exactly the evaluation setting as in [20] (i.e., same data splits, entity and relation categories). The baselines reported are:

1. SYMMETRIC STACKED ATTENTION SHIFTING (SSAS): [20] An iterative model that localizes the relationship entities using attention shift component learned for each relation.
2. SPATIAL SHIFTS [22]: Same as SSAS, but with no iterations and by replacing the shift attention mechanism with statistically learned shift per relation that ignores the semantic meaning of entities.
3. CO-OCCURRENCE [7]: Uses an embedding of the subject and object pair for attending over the image features.
4. VISUAL RELATIONSHIP DETECTION (VRD) [25]: Similar to Co-Occurrences model, but with an additional relationship embedding.

6.7. Results

Table 1 provides average IOU for Subject and Object over the three datasets described in 6.2. We com-

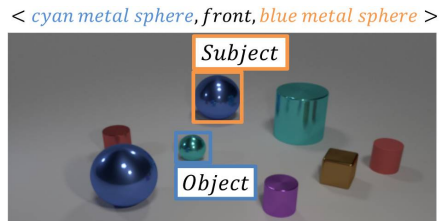


Figure 5. Typical example in CLEVR [14] dataset.

pare our model to four baselines described in 6.6. Our Differentiable Scene-Graph approach outperforms all baselines in terms of the average IOU.

Our results for the CLEVR dataset are significantly better than those in [20]. Detection in CLEVR is very easy (See Fig 5) which makes it easy to achieve high IOU. Our baseline model without the DSG layer (DSG-SG) is an end-to-end model with a two-stage detector in contrast to [20] and already improves strongly over prior work with 93.7%, and our novel DSG approach further improves to 96.3% (reducing error by 50%).

Table 2 provides results of the ablation study for the Visual Genome dataset [21].⁵ All model variants based on scene representation perform better than the model that does not use scene-graphs (i.e., DSG -SG) in terms of average IOU over subject and object, demonstrating the power of contextualized scene representation.

The full DSG model outperforms all model ablations, illustrating the improvements achieved by using partial supervision for training the differentiable scene-graph. Finally, Fig. 4 shows some success and failure cases for our DSG model, and Fig. 6 shows that the box refinement step is indeed effective.

7. Related Work

Graph Neural Networks: Recently, major progress has been made in constructing graph neural networks (GNN). These refer to a class of neural networks that operate directly on graph-structured data by passing local messages [8, 23]. Variants of GNNs have been shown to be highly effective at relational reasoning tasks [35], classification of graphs [3, 4, 29, 5], and classification of nodes in large graphs [18, 10]. The expressive power of GNNs has also been studied in [11, 42]. GNNs have also been applied to visual understanding in [11, 38, 36] and control [34, 2]. Similar aggregation schemes have also been applied to object detection [12].

Visual Relationships: Earlier work aimed to leverage visual relationships for improving detection [33], action recognition and pose estimation [6], semantic image segmentation [9] or detection of human-object interactions

⁵The numbers are different from Table 1 because Table 2 uses the validation set.

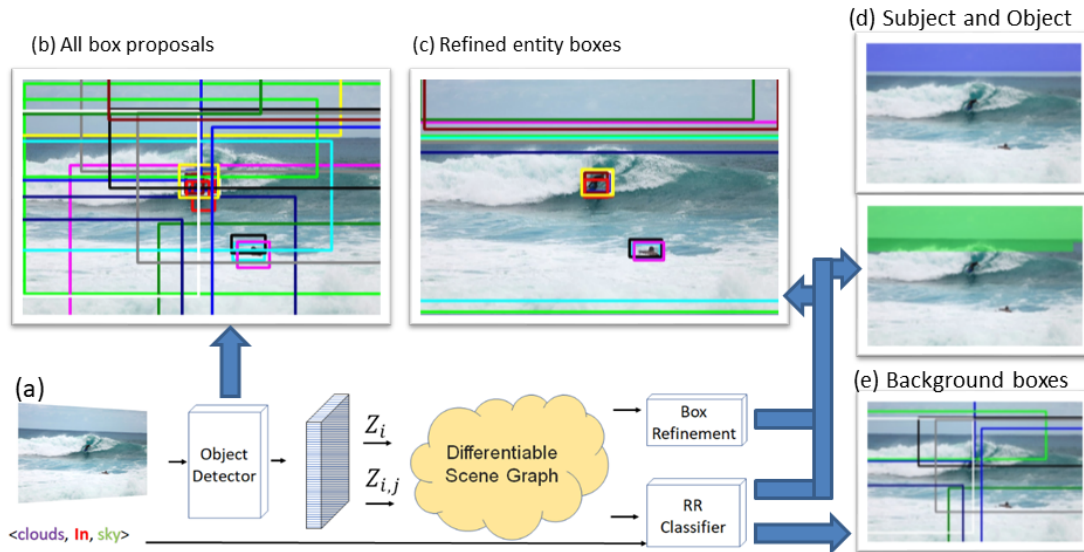


Figure 6. The effect of box refinement and RR-classification on refining bounding boxes. (a) The DSG network is applied to an input image. (b) The *object detector component* generates box proposals for entities in the image. (c) The *referring relationship classifier* uses information from DSG to label candidate boxes as *object* or *subject* entities. Then, the *box refinement component* also uses DSG information, this time to improve box locations for those boxes labeled as entities by RR. Here, boxes are tuned to focus on the most relevant entities in the image: the two men, the surfboard, the sky and the ocean. (d) Once the RR classifier labeled entity boxes, it can correctly refer to the entities in the query $\langle \text{cloud}, \text{in}, \text{sky} \rangle$ (sky in green, clouds in violet). (e) Examples of candidate boxes classified by RR as *background* (non-entity), allowing to skip them when answering queries.

[39, 30]. Lu *et al.* [25] were the first to formulate detection of visual relationships as a separate task. They learn a likelihood function that uses a language prior based on word embeddings for scoring visual relationships and constructing scene graphs.

Scene Graphs: Scene graphs provide a compact representation of the semantics of an image, and have been shown to be useful for semantic-level interpretation and reasoning about a visual scene [13]. Extracting scene graphs from images provides a semantic representation that can later be used for reasoning, question answering [40], and image retrieval [15, 31].

Another work on scene graph predictions used neural message passing algorithms [37], while [28] suggested to predict graphs directly from pixels in an end-to-end manner. NeuralMotif [43] employs an RNN that provides global context by reading sequentially the independent predictions for each entity and relation and then refines those predictions.

Referring Relationships: Several recent studies looked into the task of detecting an entity based on a referring expression [17, 19], while taking context into account. [26] described a model that has two parts: one for generating expressions that point to an entity in a discriminative fashion and a second for understanding these expressions and detecting the referred entity. [41] explored the role of context and visual comparison with other entities in referring

expressions.

Modelling context was also the focus of [27], using a multi-instance-learning objective. Recently, [20] introduced an explicit iterative model that localizes the two entities in the referring relationship task, conditioned on one another using attention from one entity to another. However, in contrast to this work, we show an implicit model that uses latent scene context, resulting in new state of the art results on three vision datasets that contain visual relationships.

8. Conclusion

Our motivation for this work is the assumption that accurate image-understanding requires a detailed representation of many entities in an image and their relations. A scene-graph is a natural structure for representing this information, but it is hard to train these in a fully supervised manner. Thus, here we advocate using a scene-graph representation that is continuous and that can also be trained from partial supervision. Our results, both qualitative (e.g., Fig. 3) and quantitative suggest that the differentiable scene-graph does encode scene structure, and that this can be used for downstream tasks such as referring relationships.

One natural next step is to study such representations in other downstream tasks that require integrating information across the image. Some examples are caption generation and visual question answering. In the latter in particular a

scene-graph could be very useful, as many questions of interest are easily answerable by scene graphs (e.g., counting questions and questions about relations).

Another important extension is to scene-graphs that also model higher order interactions (i.e., hyper-graphs).

Finally, it will be interesting to explore other approaches to training the scene-graph component, and in particular finding ways of using unlabeled data for this task.

References

- [1] S. Antol, A. Agrawal, J. Lu, M. Mitchell, D. Batra, C. L. Zitnick, and D. Parikh. VQA: visual question answering. *CoRR*, abs/1505.00468, 2015. [2](#)
- [2] P. W. Battaglia, J. B. Hamrick, V. Bapst, A. Sanchez-Gonzalez, V. F. Zambaldi, M. Malinowski, A. Tacchetti, D. Raposo, A. Santoro, R. Faulkner, Ç. Gülçehre, F. Song, A. J. Ballard, J. Gilmer, G. E. Dahl, A. Vaswani, K. Allen, C. Nash, V. Langston, C. Dyer, N. Heess, D. Wierstra, P. Kohli, M. Botvinick, O. Vinyals, Y. Li, and R. Pascanu. Relational inductive biases, deep learning, and graph networks. *CoRR*, abs/1806.01261, 2018. [7](#)
- [3] J. Bruna and S. Mallat. Invariant scattering convolution networks. *Pattern Analysis and Machine Intelligence, IEEE Transactions on*, 35(8):1872–1886, 2013. [7](#)
- [4] H. Dai, B. Dai, and L. Song. Discriminative embeddings of latent variable models for structured data. In *Int. Conf. Mach. Learning*, pages 2702–2711, 2016. [7](#)
- [5] M. Defferrard, X. Bresson, and P. Vandergheynst. Convolutional neural networks on graphs with fast localized spectral filtering. In *Neural Inform. Process. Syst.*, pages 3837–3845, 2016. [7](#)
- [6] C. Desai and D. Ramanan. Detecting actions, poses, and objects with relational phraselets. In *ECCV*, pages 158–172, 2012. [7](#)
- [7] C. Galleguillos, A. Rabinovich, and S. Belongie. Object categorization using co-occurrence, location and appearance. In *2008 IEEE Conference on Computer Vision and Pattern Recognition*, pages 1–8, June 2008. [7](#)
- [8] J. Gilmer, S. S. Schoenholz, P. F. Riley, O. Vinyals, and G. E. Dahl. Neural message passing for quantum chemistry. *arXiv preprint arXiv:1704.01212*, 2017. [7](#)
- [9] A. Gupta and L. S. Davis. Beyond nouns: Exploiting prepositions and comparative adjectives for learning visual classifiers. In *ECCV*, pages 16–29, 2008. [7](#)
- [10] W. Hamilton, Z. Ying, and J. Leskovec. Inductive representation learning on large graphs. In *Neural Inform. Process. Syst.*, pages 1024–1034, 2017. [7](#)
- [11] R. Herzig, M. Raboh, G. Chechik, J. Berant, and A. Globerson. Mapping images to scene graphs with permutation-invariant structured prediction. In *Advances in Neural Information Processing Systems (NIPS)*, 2018. [1](#), [3](#), [4](#), [7](#)
- [12] H. Hu, J. Gu, Z. Zhang, J. Dai, and Y. Wei. Relation networks for object detection. In *Proceedings of the IEEE Conference on Computer Vision and Pattern Recognition*, pages 3588–3597, 2018. [7](#)
- [13] J. Johnson, A. Gupta, and L. Fei-Fei. Image generation from scene graphs. *arXiv preprint arXiv:1804.01622*, 2018. [1](#), [8](#)
- [14] J. Johnson, B. Hariharan, L. van der Maaten, L. Fei-Fei, C. L. Zitnick, and R. B. Girshick. CLEVR: A diagnostic dataset for compositional language and elementary visual reasoning. *CoRR*, 2016. [2](#), [5](#), [7](#)
- [15] J. Johnson, R. Krishna, M. Stark, L. Li, D. A. Shamma, M. S. Bernstein, and F. Li. Image retrieval using scene graphs. In *Proc. Conf. Comput. Vision Pattern Recognition*, pages 3668–3678, 2015. [1](#), [8](#)
- [16] J. Johnson, R. Krishna, M. Stark, L.-J. Li, D. Shamma, M. Bernstein, and L. Fei-Fei. Image retrieval using scene graphs. In *Proceedings of the IEEE Conference on Computer Vision and Pattern Recognition*, pages 3668–3678, 2015. [1](#)
- [17] S. Kazemzadeh, V. Ordonez, M. Matten, and T. Berg. Referitgame: Referring to objects in photographs of natural scenes. In *Proceedings of the 2014 conference on empirical methods in natural language processing (EMNLP)*, pages 787–798, 2014. [2](#), [8](#)
- [18] T. N. Kipf and M. Welling. Semi-supervised classification with graph convolutional networks. *CoRR*, abs/1609.02907, 2016. [7](#)
- [19] E. Krahmer and K. Van Deemter. Computational generation of referring expressions: A survey. *Computational Linguistics*, 38(1):173–218, 2012. [2](#), [8](#)
- [20] R. Krishna, I. Chami, M. Bernstein, and L. Fei-Fei. Referring relationships. In *IEEE Conference on Computer Vision and Pattern Recognition*, 2018. [2](#), [5](#), [6](#), [7](#), [8](#)
- [21] R. Krishna, Y. Zhu, O. Groth, J. Johnson, K. Hata, J. Kravitz, S. Chen, Y. Kalantidis, L.-J. Li, D. A. Shamma, M. Bernstein, and L. Fei-Fei. Visual genome: Connecting language and vision using crowdsourced dense image annotations. *ArXiv e-prints*, 2016. [2](#), [5](#), [7](#)
- [22] D. LaBerge, R. Carlson, J. Williams, and B. Bunney. Shifting attention in visual space: tests of moving-spotlight models versus an activity-distribution model. *Journal of experimental psychology. Human perception and performance*, 23(5):13801392, October 1997. [7](#)
- [23] Y. Li, D. Tarlow, M. Brockschmidt, and R. S. Zemel. Gated graph sequence neural networks. *CoRR*, abs/1511.05493, 2015. [7](#)
- [24] W. Liao, M. Y. Yang, H. Ackermann, and B. Rosenhahn. On support relations and semantic scene graphs. *arXiv preprint arXiv:1609.05834*, 2016. [1](#)
- [25] C. Lu, R. Krishna, M. S. Bernstein, and F. Li. Visual relationship detection with language priors. In *European Conf. Comput. Vision*, pages 852–869, 2016. [2](#), [5](#), [7](#), [8](#)
- [26] J. Mao, J. Huang, A. Toshev, O. Camburu, A. L. Yuille, and K. Murphy. Generation and comprehension of unambiguous object descriptions. In *Proceedings of the IEEE conference on computer vision and pattern recognition*, pages 11–20, 2016. [8](#)
- [27] V. K. Nagaraja, V. I. Morariu, and L. S. Davis. Modeling context between objects for referring expression understanding. In *European Conference on Computer Vision*, pages 792–807. Springer, 2016. [8](#)

- [28] A. Newell and J. Deng. Pixels to graphs by associative embedding. In *Advances in Neural Information Processing Systems 30 (to appear)*, pages 1172–1180. Curran Associates, Inc., 2017. 8
- [29] M. Niepert, M. Ahmed, and K. Kutzkov. Learning convolutional neural networks for graphs. In *Int. Conf. Mach. Learning*, pages 2014–2023, 2016. 7
- [30] B. A. Plummer, A. Mallya, C. M. Cervantes, J. Hockenmaier, and S. Lazebnik. Phrase localization and visual relationship detection with comprehensive image-language cues. In *ICCV*, pages 1946–1955, 2017. 8
- [31] D. Raposo, A. Santoro, D. Barrett, R. Pascanu, T. Lillicrap, and P. Battaglia. Discovering objects and their relations from entangled scene representations. *arXiv preprint arXiv:1702.05068*, 2017. 8
- [32] S. Ren, K. He, R. B. Girshick, and J. Sun. Faster R-CNN: towards real-time object detection with region proposal networks. *CoRR*, abs/1506.01497, 2015. 3
- [33] M. A. Sadeghi and A. Farhadi. Recognition using visual phrases. In *Computer Vision and Pattern Recognition (CVPR)*, 2011. 7
- [34] A. Sanchez-Gonzalez, N. Heess, J. T. Springenberg, J. Merel, M. A. Riedmiller, R. Hadsell, and P. Battaglia. Graph networks as learnable physics engines for inference and control. In *ICML*, pages 4467–4476, 2018. 7
- [35] A. Santoro, D. Raposo, D. G. Barrett, M. Malinowski, R. Pascanu, P. Battaglia, and T. Lillicrap. A simple neural network module for relational reasoning. In *Neural Inform. Process. Syst.*, pages 4967–4976, 2017. 7
- [36] X. Wang and A. Gupta. Videos as space-time region graphs. In *ECCV*, 2018. 7
- [37] D. Xu, Y. Zhu, C. B. Choy, and L. Fei-Fei. Scene Graph Generation by Iterative Message Passing. In *Proc. Conf. Comput. Vision Pattern Recognition*, pages 3097–3106, 2017. 1, 8
- [38] J. Yang, J. Lu, S. Lee, D. Batra, and D. Parikh. Graph R-CNN for scene graph generation. In *European Conf. Comput. Vision*, pages 690–706, 2018. 7
- [39] M. Y. Yang, W. Liao, H. Ackermann, and B. Rosenhahn. On support relations and semantic scene graphs. *ISPRS journal of photogrammetry and remote sensing*, 131:15–25, 2017. 8
- [40] K. Yi, J. Wu, C. Gan, A. Torralba, P. Kohli, and J. Tenenbaum. Neural-symbolic vqa: Disentangling reasoning from vision and language understanding. In *Advances in Neural Information Processing Systems*, pages 1039–1050, 2018. 8
- [41] L. Yu, P. Poirson, S. Yang, A. C. Berg, and T. L. Berg. Modeling context in referring expressions. In *European Conference on Computer Vision*, pages 69–85. Springer, 2016. 8
- [42] M. Zaheer, S. Kottur, S. Ravanbakhsh, B. Póczos, R. R. Salakhutdinov, and A. J. Smola. Deep sets. In *Advances in Neural Information Processing Systems 30*, pages 3394–3404. Curran Associates, Inc., 2017. 7
- [43] R. Zellers, M. Yatskar, S. Thomson, and Y. Choi. Neural motifs: Scene graph parsing with global context. *arXiv preprint arXiv:1711.06640*, abs/1711.06640, 2017. 1, 8
- [44] J. Zhang, K. J. Shih, A. Tao, B. Catanzaro, and A. Elgammal. An interpretable model for scene graph generation. *CoRR*, abs/1811.09543, 2018. 1